Development of Functionally Graded Material Capabilities in Large-scale Extrusion Deposition Additive Manufacturing

James Brackett[1], Yongzhe Yan[2], Dakota Cauthen[3], Vidya Kishore[4], John Lindahl[4], Tyler Smith[3,4], Haibin Ning[2], Vlastamil Kunc[3,4], Chad Duty[3,4]

[1] Energy Science and Engineering, University of Tennessee – Knoxville, TN
[2] Materials Science and Engineering, University of Alabama – Birmingham, AL
[3] Mechanical, Aerospace, and Biomedical Engineering, University of Tennessee – Knoxville, TN
[4] Manufacturing Demonstration Facility, Oak Ridge National Laboratory, TN

Abstract

Additive manufacturing's (AM) layer-by-layer nature is well-suited to the production of Functionally Graded Materials (FGM) with discrete material boundaries. Extrusion deposition is especially advantageous since multiple nozzles easily accommodate the inclusion of additional materials. However, discrete interfaces and sudden composition changes can limit the functionality of a printed part through inherently weak bonding. Furthermore, same-layer transitions are not only difficult to execute, but also further amplify structural weaknesses by creating multiple discrete interfaces. Therefore, successfully implementing a blended, continuous gradient will greatly advance the applicability of FGM in additive manufacturing. The pellet-fed nature and integrated screw design of the Big Area Additive Manufacturing system enables material mixing needed for development of this capability. Using constituent content analysis, this study evaluates the transition behavior of a neat ABS/CF-ABS material pair and characterizes the repeatability of the mixing and printing process, which ultimately leads to control of site-specific material deposition and properties.

Introduction

Additive manufacturing (AM) capabilities have been continuously expanded in recent years, and its potential for industrial applications has maintained a high level of interest. One of several areas being fervently explored is the adapting current processes to produce Multi-Material (MM) and Functionally Graded Material (FGM) structures. While many AM systems were developed for single-material use, Multi-Material Additive Manufacturing (MMAM) provides increased functionality. A process is generally considered to truly be MMAM only if it utilizes more than one material and does not require pre-mixing, pre-compositing, or non-AM post-processing treatment [1]. On the contrary, an FGM can be constructed through one or more materials and is most accurately characterized by a spatial variation in composition or densification to achieve a desired functional performance [2]. Within this definition lie two classifications of FGM's: stepwise and continuous. A stepwise FGM relies on a multi-layered approach with discrete interfaces appearing periodically through the structure to create an overarching structure change via regions of differing microstructures. A continuous FGM, however, exhibits a constant change in microstructural composition across the occupied spatial region [3].

MMAM has been explored in recent years with a variety of processes and methods, but the majority still tend to produce MM structures by assigning different materials to different layers. This approach experiences issues associated with the difficulty of bonding dissimilar materials. For example, production of a sandwich structure with a Stratasys PolyJet Connex 350 system utilizing an adhesives-based approach and T-Peel geometry found that fracture consistently occurred at material interfaces [4]. Although further investigation demonstrated that aligning the material interface perpendicular to build direction improved fracture resistance along the interface, it did not completely eliminate the interface vulnerability [5]. Similarly, Brischetto et al investigated sandwich structure configurations produced with a multi-nozzle Fused Filament Fabrication (FFF) Sharebot NG 3D printer. Their work concluded that a fully single-material PolyLactic Acid (PLA) structure outperformed one that substituted ABS for the external face sheets when suing a honeycomb core. Implementing a solid PLA core improved performance, leading them to suggest both poor adhesion and premature cooling due to nozzle switching is to blame [6]. Roger et al explored three techniques for improving the interface strength between differently-colored ABS, and while an interpenetrating pattern where each layer's interface boundary is shifted from one side to another did improve ultimate tensile strength, the configuration still significantly underperformed compared to single-material constructions [7]. Another approach assessed the influence of structural arrangement of the ABS and PLA regions on mechanical performance. Kim et al found that incorporating material changes in both the print direction and the z-direction dramatically improved performance and assisted to limit the detrimental influence of void formation between dissimilar beads [8].

Application of MMAM technology to incorporate FGM into AM has also been prevalent. Vu et al further expanded their MMAM T-peel investigations to incorporate a stepwise FGM, which exhibited a significant increase in peel force and apparent fracture energy compared to a simple sandwich structure geometry [5]. Stratasys's PolyJet technology was also implemented in construction of a soft, flexible robot shell to create an FGM that varied in elastic modulus from 1 MPa to 1 GPa, which allowed it to soften impacts while maintaining a semi-rigid overall shape and survive longer than its purely rigid or flexible counterparts [9]. Stratasys has also developed partnerships intended to attack the problem from the software side. Ezair et al developed a software interface that allows designers to volumetrically apply material choices to their designs instead of relying on contemporary boundary-representation techniques. With this framework, the team produced FGM structures that demonstrated control of porous regions and deposition of differing materials via repeatable patterns [10]. Investigation of FGM has even been conducted with large-scale AM. In one such study, Cincinnati's Big Area Additive Manufacturing (BAAM) system was used to print two different types of stepwise FGM sandwich structures, which demonstrated the potential for FGM implementation to impart both cost and weight savings even within AM [11].

The goal of this investigation is to expand upon the initial BAAM work and investigate the implantation of a continuous FGM in large-scale AM. In particular, it will characterize the continuous transition produced by in-situ material switching during printing. The BAAM at Oak Ridge National Laboratory's Manufacturing Demonstration Facility provides a unique opportunity for this study due to recent alterations enabling a dual-hopper configuration while printing, which allows for on-the-fly material switching made possible by the pelletized feedstock and extrusion system. This set-up provides significant advantages over multi-nozzle

systems given the inherent blending of a screw-based extruder and the lack of stoppage during material switching. For this investigation, carbon fiber reinforced ABS and neat ABS are chosen as the bi-material system. Maintaining the same polymer matrix between the two materials allows for the printing process to be characterized with minimal outside factors.

Experimental

Two grades of ABS were obtained in a pelletized form from Techmer Engineered Solutions. The first was a Neat ABS (HIFILL ABS 1000 3DP)) and the second was a 20 wt. % carbon fiber ABS (Electrafil J-1200/CF/20 3DP). Both materials were used in printing on the Manufacturing Demonstration Facility's (MDF) Big Area Additive Manufacturing (BAAM) – B that features an innovative dual-hopper system for multi-material printing. Seen in Figure 1, the system functions on a rocker mechanism that forces one hopper's feeding tube closed and off the barrel while simultaneously opening and moving the other into position. The materials were dried at 85°C overnight prior to printing.

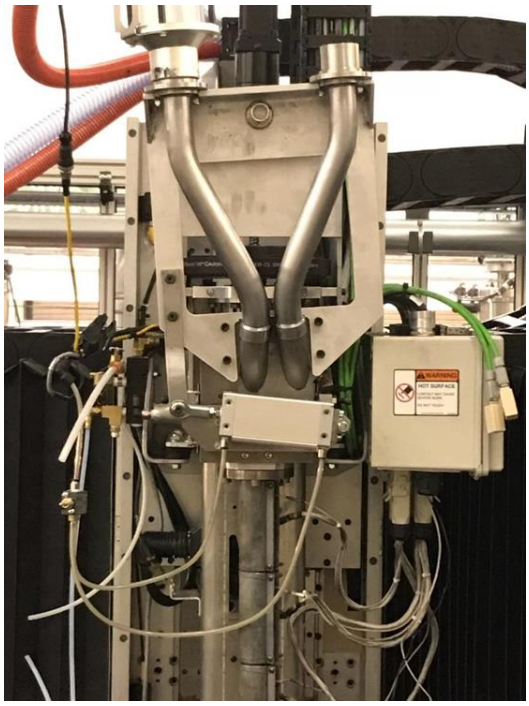

Figure 1: The newly installed dual-hopper system on the MDF's BAAM-B. This system enables in-situ material switching for MM and FGM large-scale printing of thermoplastics.

Printing Plan and Parameters

To demonstrate a complete material transition from in-situ feedstock switching, the single-walled rectangle geometry in Figure 2A was chosen. By implementing a hopper switch twice within a layer at opposing corners, a complete transition was confined to the long sides of a rectangle with dimensions 11.5 ft by 5 ft. The printing process for a single print consisted of three stages: an initial single-layer that was printed and removed, a 20-layer rectangle that was printed and removed, then a final single-layer was printed and removed. No purging was

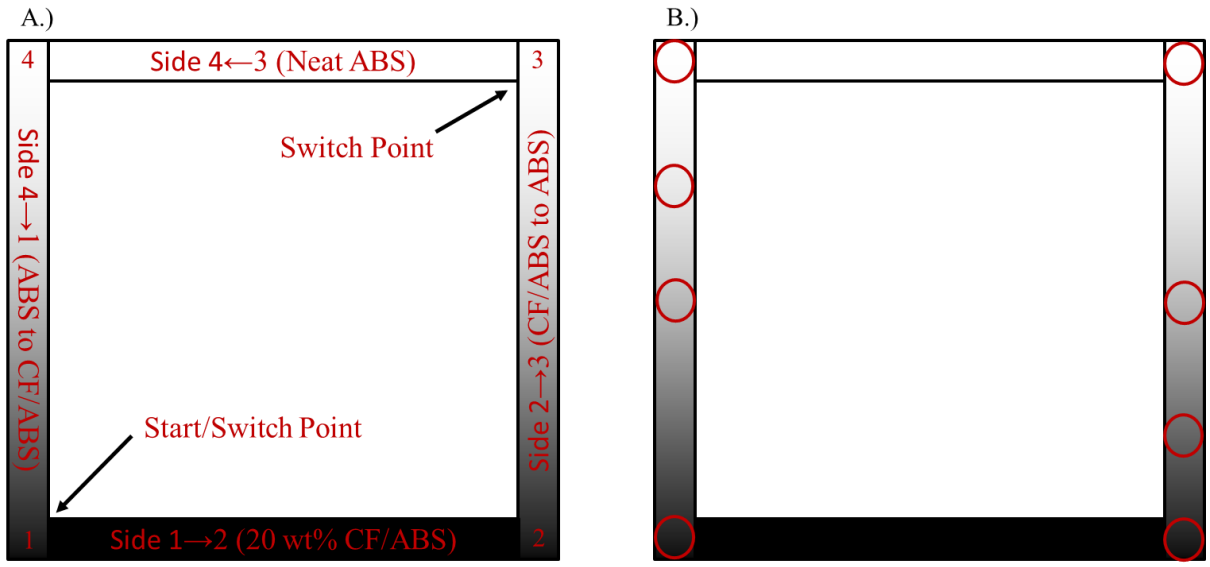

Figure 2: A.) Schematic of the printed rectangle. The expected composition of each side is indicating with labels, and the corners marked 1 and 3 label the two points within a layer that a material switch was initiated. B.) The 4 locations along each side where samples were extracted.

conducted between stages. The purpose of the 20-layer stage is merely to incorporate numerous in-situ switches over the lifecycle of a print so that the effects of continual switching on the transition in a later layer can be observed. In total, three prints were conducted and analyzed to identify the consistency of the material switch, the repeatability of the transition throughout the layers of a print, and the repeatability of the transition in after multiple prints. Furthermore, the impact of transition direction (Material A → Material B vs. Material B → Material A) will be evident by comparing opposing sides of the rectangle.

These prints utilized a nozzle of 10.16 mm (0.4 in) diameter with a non-mixing screw. The print parameters maintained a constant screw speed of 300 RPM with travel speed of 106.7 mm (4.2 in/s) with layer height 6.35 mm (0.25 in), bead width 15.24 mm (0.6 in), melt temperature of 245°C, and bed temperature of 100°C.

Constituent Content Analysis

Tracking the transition from one material to the next requires determination of material composition at any given point. For this material pair, wt % carbon fiber is used to track the change between materials. ASTM D3171 Procedure H: Carbonization in Nitrogen (CIN) protects the carbon fibers with an inert nitrogen atmosphere while eliminating the polymer matrix [12]. Additionally, it implements a 100% Neat ABS control to ensure any remaining debris from polymer burn-off is considered. A Lindberg Blue M nitrogen tube furnace was used to conduct Procedure H. The remaining percent carbon fiber is compared to the nominal constituent content of the 20% CF/ABS, which was found to be closer to 21 wt % carbon fiber. All mass measurements were taken with Mettler Toledo Balance, XS204 Deltarange to a 0.1 mg accuracy.

To ensure accurate data, each single-layer rectangle was sectioned into 152.4 mm (6 in) rods and labeled to indicate the order and direction of the print. Using an Isomet 1000 Precision Saw, samples 8.4 mm in length were taken from the ends of these rods at the desired locations, which were chosen so that samples from different layers and prints would maintain the same distance from most recent switch for direct comparison. As can be seen in Figure 2B, each sample set consisted of four locations on each side chosen such that both neat and transition regions would be represented.

CIN testing was divided into four categories to determine the consistency of the transition, repeatability of the printing, repeatability of layers, and the construction of the transition curve. In the first set of experiments, three consecutive samples were taken to confirm that CIN yields the same fiber content for each one, thus testing for any variance in the procedure or during a given transition. Variance between different prints of the same structure were then considered to ensure that a transition is predictable and repeatable. In the third experimental set, the first and final layers are compared to establish if continuous switching throughout a print causes a change in the transition behavior. Finally, numerous additional samples were taken from a single print to construct a beginning to end transition curve that describes the switch from CF/ABS to Neat ABS and back.

Results and Discussion

Repeatability of Sampling Location

Figure 3 shows the CIN results of subsequent samples at four locations for both transition directions. Three locations required additional testing, for while they showed consistency in measurement, there was an issue with the control sample that initially returned negative values. The repeat testing utilized only one sample to obtain a reasonable fiber measurement as the original measurements had already proven consistency. Additionally, the 1.98 m location in Figure 3A initially showed a significant difference in the three samples from that spot, but repeat testing confirmed that the two of the measurements were anomalies. Thus, Figure 3A and 3B demonstrate that the material transition is consistent. Moving forward, it allows for the treatment of single 8.4 mm sample as representative of the surrounding area.

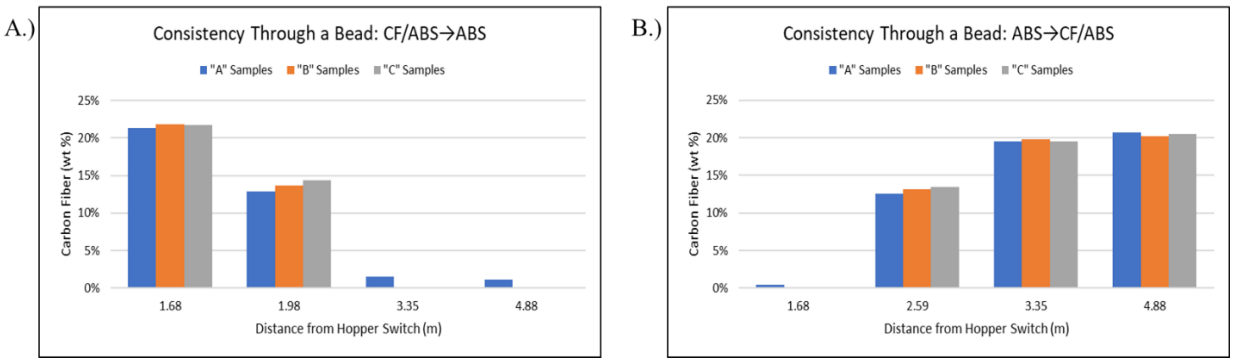

Figure 3: The carbon fiber content of three consecutive 8.4 mm samples taken from four locations along the A.) CF/ABS to ABS transition and B.) the ABS to CF/ABS transition.

Repeatability of the Printing

Figure 4 shows the resulting fiber content as measured by CIN for each of the three prints in both transition directions. For both directions and all locations, the variation in measured fiber content is minimal. The maximum fiber wt % difference observed between measurements is less than 1.5 wt %, and the largest standard deviation at a location was 0.66%. This indicates the in-situ switching process can be reliably charted and replicated between prints, which will allow for accurate modelling and application of a shape function to the printing process.

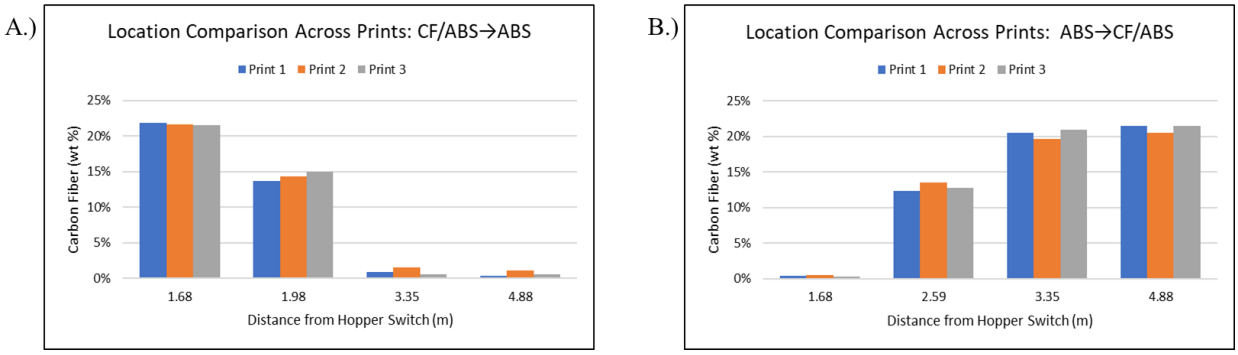

Figure 4: The carbon fiber content at four specified distances from where the hopper switch was initiated for the A.) CF/ABS to ABS transition and B.) the ABS to CF/ABS transition.

Repeatability of Layers

Figure 5 contains the fiber content measured via CIN for layers 1 and 20 in both transition directions at four locations each. Figure 5a shows consistent fiber content for locations outside of the transition, however, the location within the transitioning region consistently illustrated a difference between the layers. Fiber content is lower at later layers, implying that the transition region will drift or shift to occur faster or sooner in later layers compared to initial layers. In contrast, transitioning from a neat ABS to the carbon fiber filled ABS maintained a consistent fiber content at all spots. Thus, transition drift appears to be transition direction dependent and is heavily influenced by the presence of fiber fillers. A possible explanation is the build-up of residual fibers inside the barrel of the extruder assisting in a rapid change to CF/ABS. For example, even after fiber content drops below 1% and reaches steady state, the neat ABS portion still shows a visible fiber presence, as seen in Figure 5b. While the exact mechanism is not clear, the residual fibers are a likely source.

A.)

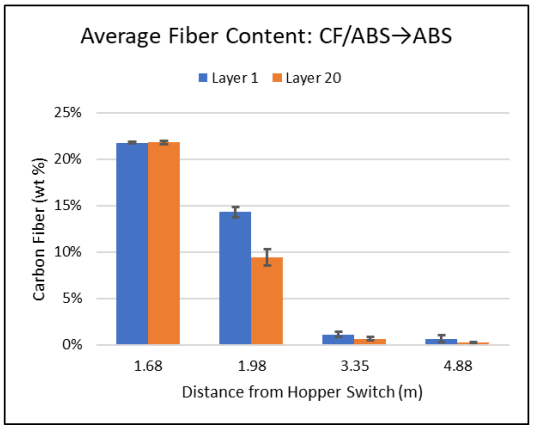

B.)

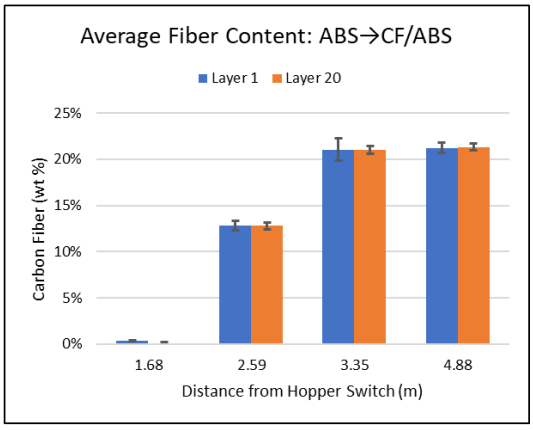

Figure 5: The average fiber content of the three prints at each of the four locations for both the first and the last layer printed. A.) The CF/ABS to ABS transition and B.) The ABS to CF/ABS transition.

Transition Curves

Establishing confidence in the in-situ switching print capability as a repeatable process provided the needed support for analysis of a single print's transitions as representative of the material pair's behavior. Thus, additional data points taken from locations before, during, and after the transition were utilized to map the change in fiber content through the printed bead. Figure 6 shows the change in fiber content over distance for the transition from 20 wt % CF/ABS to Neat ABS. Due to the behavior it exhibited, the transition was divided into three distinct regions. The first, the "Purge Zone", consists of the first material due to the time it takes for the initial traces of the new material to travel from the top of the extruder through the barrel and to the nozzle. At this point, it enters the "Transition Zone," where the carbon fiber content continuously changes until reaching a stable level associated with the second material, the "Steady State Zone." In comparison to Figure 7, it is evident that the directionality of the transition imparts different characteristics into the transition. Figure 8 combines the two graphs to more easily illustrate that the two transitions are not simply reversible, implying that the direction of the transition should be included as another parameter.

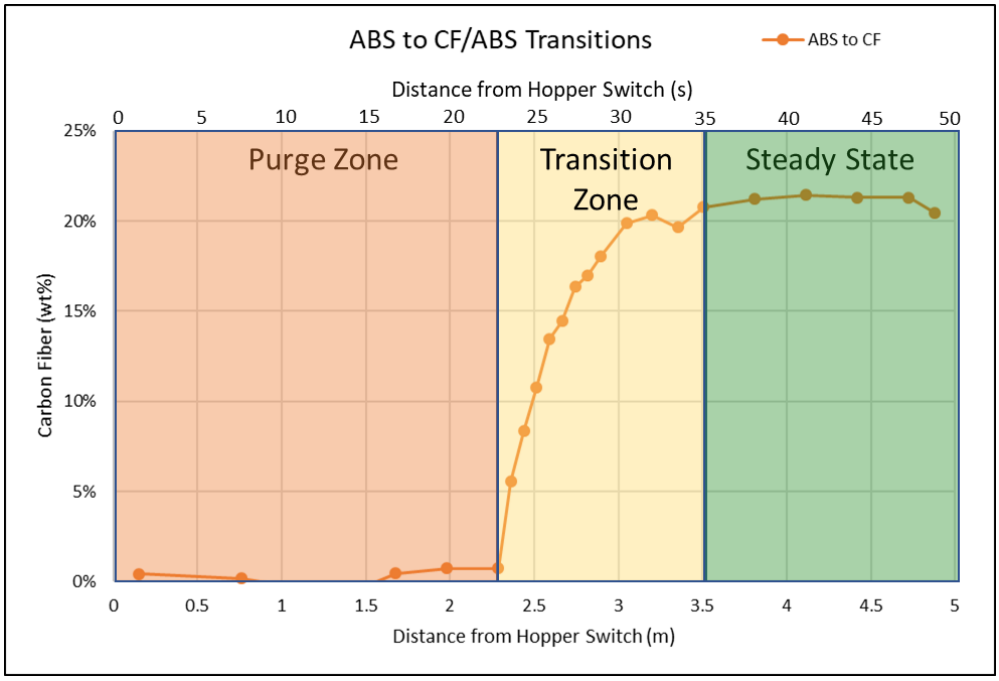

Figure 6: The change in fiber content over time (s) and distance(m) from Neat ABS to 20 wt % CF/ABS. More measurements were taken in the transition zone for improved resolution.

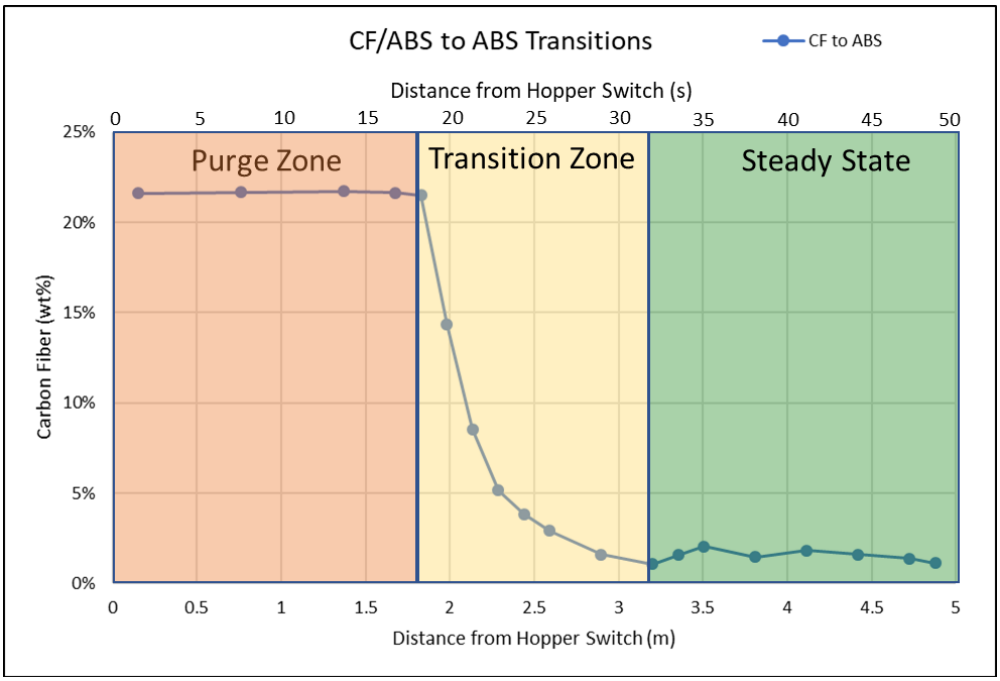

Figure 7: The change in fiber content over time (s) and distance(m) from 20 wt % CF/ABS to Neat ABS. More measurements were taken in the transition zone for improved resolution.

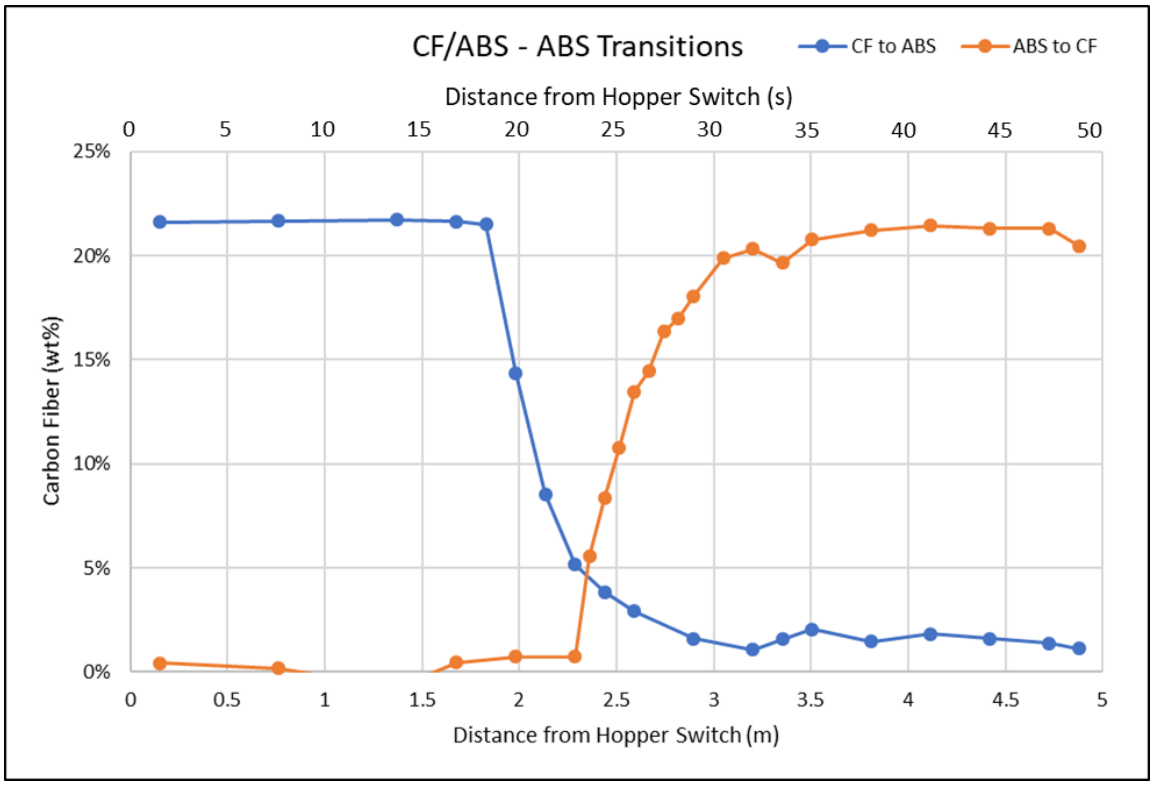

Figure 8: The CF/ABS to ABS and ABS to CF/ABS transitions overlaid on the same chart, highlighting the differences in transition behavior.

Table 1 quantifies the zones shown in Figures 6 and 7. While CF/ABS to Neat ABS demonstrates a shorter purge zone and quicker time to steady-state, the actual transition zone is slightly larger than that of the Neat ABS to CF/ABS direction. Overall, the CF/ABS to Neat ABS is a quicker process, but for both, the presence of a significant purge zone is an important distinction. For print design, it must be considered when inputting switch commands to not only ensure that steady state for Material B is reached when needed but also that the transition zone's location is properly controlled.

Table 1: Numerical comparison of Purge and Transition zones

Unit	Direction	Purge Zone	Transition Zone	Combined
Meter	CF/ABS→ABS	1.83	1.37	3.20
	ABS→CF/ABS	2.29	1.22	3.51
Second	CF/ABS→ABS	17.14	12.86	30.00
	ABS→CF/ABS	21.43	11.43	32.86

Conclusions and Future Work

Implementing an in-situ material change via feedstock switching for creation of functionally graded and multi-material structures is viable. The transition was proven to be consistent through the bead with reliable, repeatable measurements of composition possible from just a 8.4 mm (1/3 in) samples. Printing the same structure multiple times with in-situ switching

produces near-identical transition behavior. However, evidence suggests that a material pair's transition may not remain consistent after numerous switches within a single print since the CF/ABS to Neat ABS transition showed a significant difference between Layers 1 and 20 in the transition location. Conversely, transitioning in the opposite direction exhibited no change from the first layer to the twentieth, indicating that the change could be related to fiber build-up. Therefore, in-situ switching can, at the minimum, be considered a completely repeatable process for initial layers, so treatment of a single print as representative of a material pair's transition behavior is justified.

Creation of complete transition curves enabled a direct comparison of the opposite transition directions. Given that the transitions were not reversible, it indicates that the direction of a transition should also be considered a factor in predicting a material pair's transition behavior. Furthermore, the complete curves illustrated the importance of considering the time it takes for a feedstock switch to manifest in the printing process. Without proper characterization of the Purge Zone, initiating material switches within a print that accurately place the transition zone is not possible.

This investigation is the beginning of a complete characterization of the dual-hopper's FGM and MM capabilities. Moving forward, future studies will focus on quantifying the effects of various parameters. These include the directionality exhibited in this paper and what its cause is, the effect of differing screw designs and RPMS, and the influence of switching from one polymer matrix to another.

Acknowledgements

Research sponsored by the U.S. Department of Energy, Office of Energy Efficiency and Renewable Energy, Industrial Technologies Program, under contract DE-AC05-00OR22725 with UT-Battelle, LLC. Thank you to Cincinnati Incorporated for equipment and assistance. Special thanks to the University of Alabama Birmingham's Materials Science Department for their help and cooperation with testing and data collection. This work was supported in part by Oak Ridge Institute for Science and Education through the Higher Education Research Experiences Program (HERE).

References

[1] M. Vaezi, S. Chianrabutra, B. Mellor, and S. Yang, "Multiple material additive manufacturing – Part 1: a review," *Virtual & Physical Prototyping,* Article vol. 8, no. 1, pp. 19-50, 2013, doi: 10.1080/17452759.2013.778175.

[2] G. H. Loh, E. Pei, D. Harrison, and M. D. Monzón, "An overview of functionally graded additive manufacturing," *Additive Manufacturing*, vol. 23, pp. 34-44, 2018/10/01/ 2018, doi: https://doi.org/10.1016/j.addma.2018.06.023.

[3] G. Udupa, S. S. Rao, and K. V. Gangadharan, "Functionally graded Composite materials: An overview," in *International Conference on Advances in Manufacturing and Materials Engineering*, vol. 5, S. Narendranath, M. R. Ramesh, D. Chakradhar, M. Doddamani, and S. Bontha Eds., (Procedia Materials Science. Amsterdam: Elsevier Science Bv, 2014, pp. 1291-1299.

[4] I. Vu, L. Bass, N. Meisel, B. Orler, C. B. Williams, and D. A. Dillard, "Characterization of Mutli-Material Interfaces in PolyJet Additive Manufacturing," *Solid Freeform Fabrication Symposium Proceedings,* Conference Proceeding pp. 959-982, 2015.

[5] I. Q. Vu, L. B. Bass, C. B. Williams, and D. A. Dillard, "Characterizing the effect of print orientation on interface integrity of multi-material jetting additive manufacturing," *Additive Manufacturing,* vol. 22, pp. 447-461, 2018/08/01/ 2018, doi: https://doi.org/10.1016/j.addma.2018.05.036.

[6] S. Brischetto, C. Ferro, R. Torre, and P. Maggiore, "3D FDM production and mechanical behavior of polymeric sandwich specimens embedding classical and honeycomb cores," *Curved and Layered Structures,* vol. 5, pp. 80-94, 04/01 2018, doi: 10.1515/cls-2018-0007.

[7] F. Roger and P. Krawczak, *3D-printing of thermoplastic structures by FDM using heterogeneous infill and multi-materials: An integrated design-advanced manufacturing approach for factories of the future*. 2015.

[8] H. Kim, E. Park, S. Kim, B. Park, N. Kim, and S. Lee, "Experimental Study on Mechanical Properties of Single- and Dual-material 3D Printed Products," *Procedia Manufacturing,* vol. 10, pp. 887-897, 2017/01/01/ 2017, doi: https://doi.org/10.1016/j.promfg.2017.07.076.

[9] N. W. Bartlett *et al.*, "A 3D-printed, functionally graded soft robot powered by combustion," (in English), *Science,* Article vol. 349, no. 6244, pp. 161-165, Jul 2015, doi: 10.1126/science.aab0129.

[10] B. Ezair and G. Elber, "Fabricating Functionally Graded Material Objects Using Trimmed Trivariate Volumetric Representations," *Fabrication and Sculpting Event,* Conference Proceedings 2017.

[11] Z. Sudbury, C. Duty, and K. Vlastimil, "Expanding Material Property Space Maps with Functionally Graded Materials for Large Scale Additive Manufacturing," *Solid Freeform Fabrication Symposium Proceedings,* pp. 459-484, 2017.

[12] "ASTM D3171-15 Standard Test Methods for Constiuent Content of Composite Materials," *ASTM International, West Conshohocken, PA.,* ASTM Standard 2015, doi: 10.1520/D3171-15.